Supporting Information

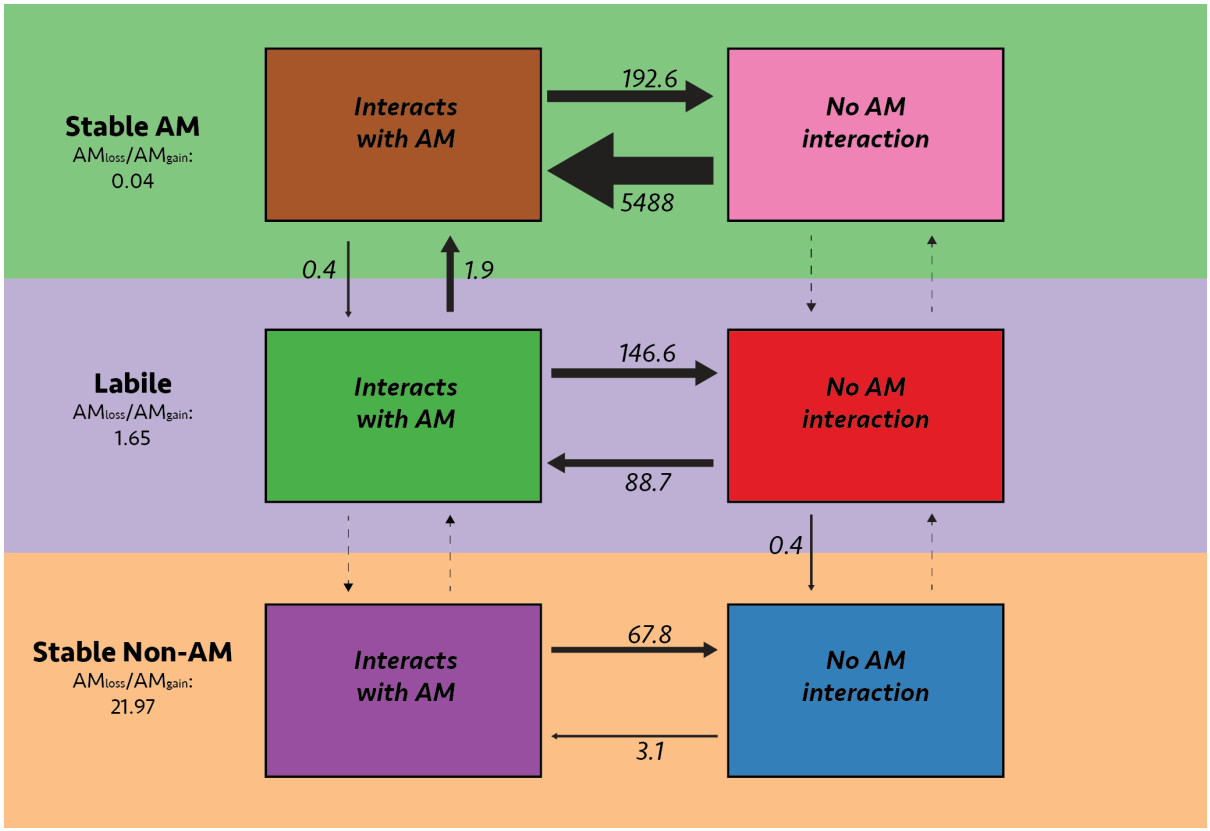

SI Figure 1: The transition rate matrix for our best model (See Table 1) reveals that there are three speeds of evolution in the history of the plant-AM mutualism: a class where AM interactions are strongly favoured (top, green background), a labile class (middle, purple background) and a class of plants where loss of AM is strongly favoured (bottom, orange background). Transitions from left to right indicate AM loss, vertical arrows indicate transitions among rate classes. Numbers below the classes indicate the AM_{loss}/AM_{gain} ratio which is a measure of the relative evolutionary stability of plant-AM interactions. The background colours indicating these three AM stability classes are plotted onto the phylogeny in SI Figure 2. Transition rates are indicated at the arrows in number of transitions per 100 million years per lineage. Dotted lines indicate transitions that were possible under the model, but where inferred to be zero. The ancestral state of spermatophytes is the brown state, i.e. a stable AM interaction.

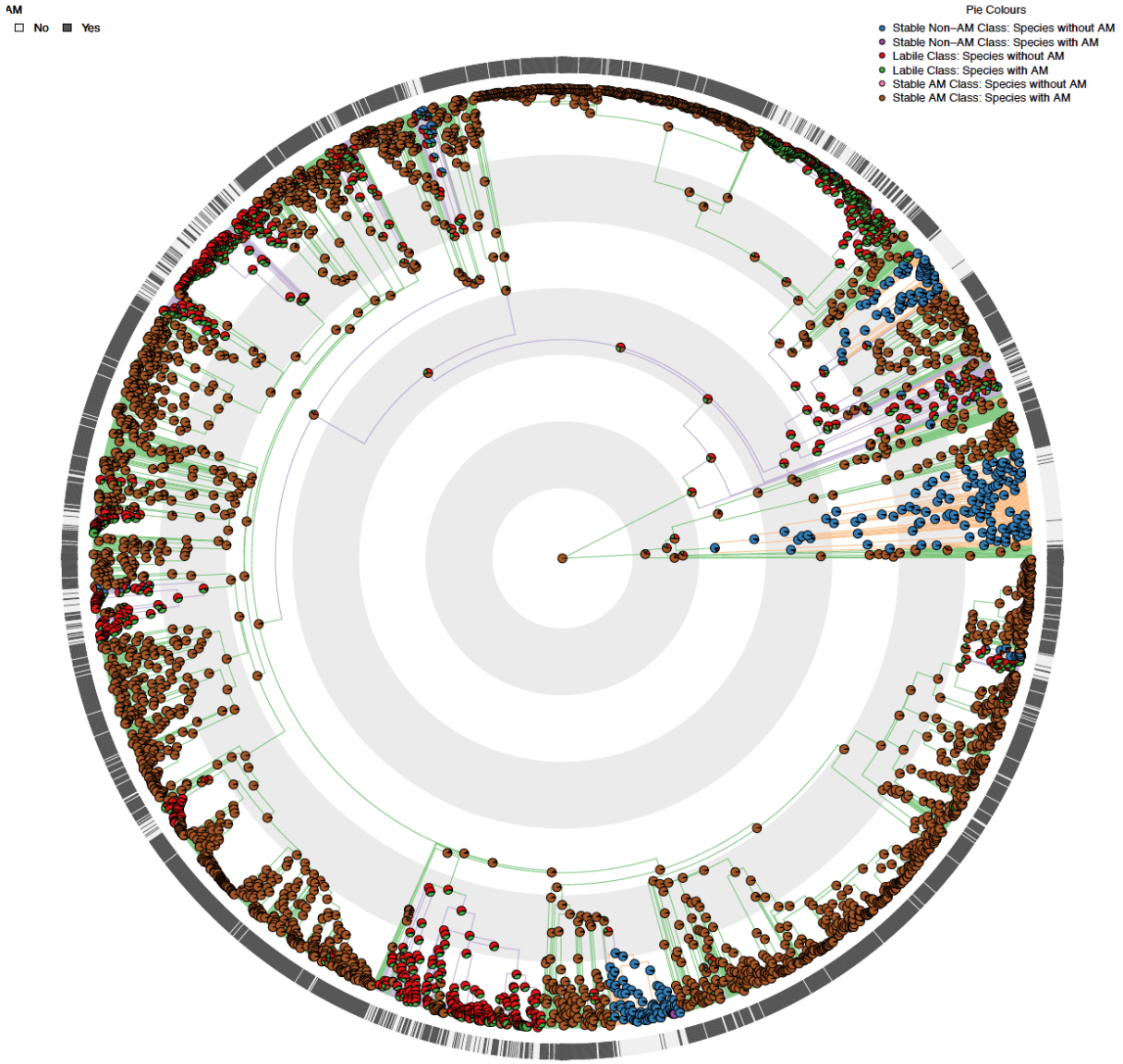

SI Figure 2: Three stability classes of the plant-AM fungal mutualism (See SI Figure 1) are found throughout the seed plants. Branches are coloured according to stability classes from SI Figure 1 (green, purple and orange pastel colours), while pie charts indicate the character state for each node also matching the colours from SI Figure 1. The coloured band around the phylogeny indicates the reported presence (dark grey) or absence of AM interactions across 3,736 species. Grey and white concentric circles indicate periods of 50 million years. An expanded version of this figure, containing fully legible species names (when zooming in) is available as a high resolution figure within SI Appendix.

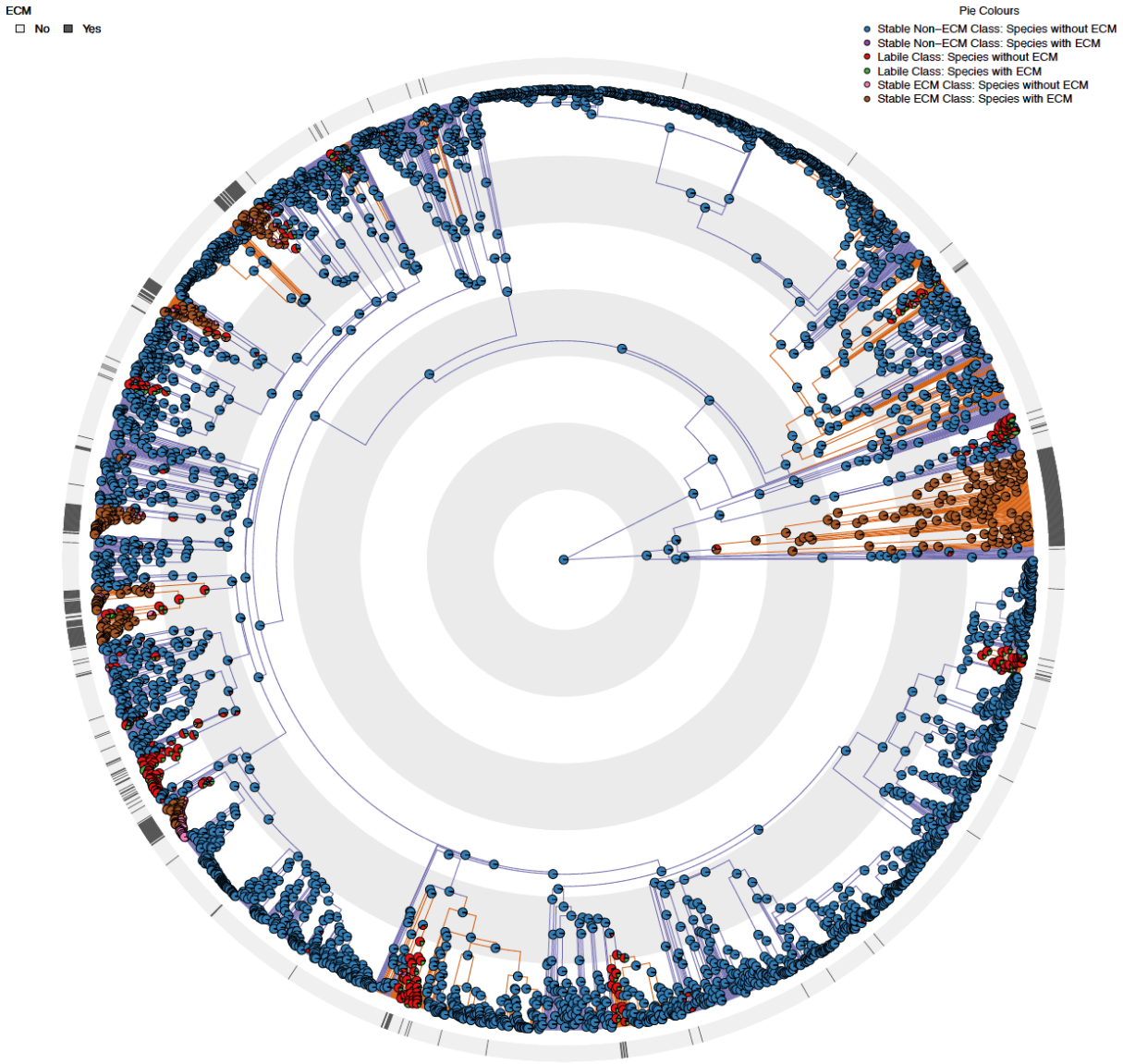

SI Figure 3: The pie charts in this figure depict the ancestral state reconstruction of plant-ectomycorrhizal fungi (ECM) interactions under the best HRM-model (SI Table 1). The coloured band across the phylogeny indicate the reported presence (dark grey) or absence of EM interactions across our 3,736 species. The branch colours indicate the reconstructed presence (purple) or absence (orange) of AM fungi under the best HRM-model for plant-AM interactions (Table 1, SI Figures 1 & 2). We visually observe that AM-loss in many cases co-occurs with an evolutionary shift to EM fungal interactions, most prominently in the Pines.

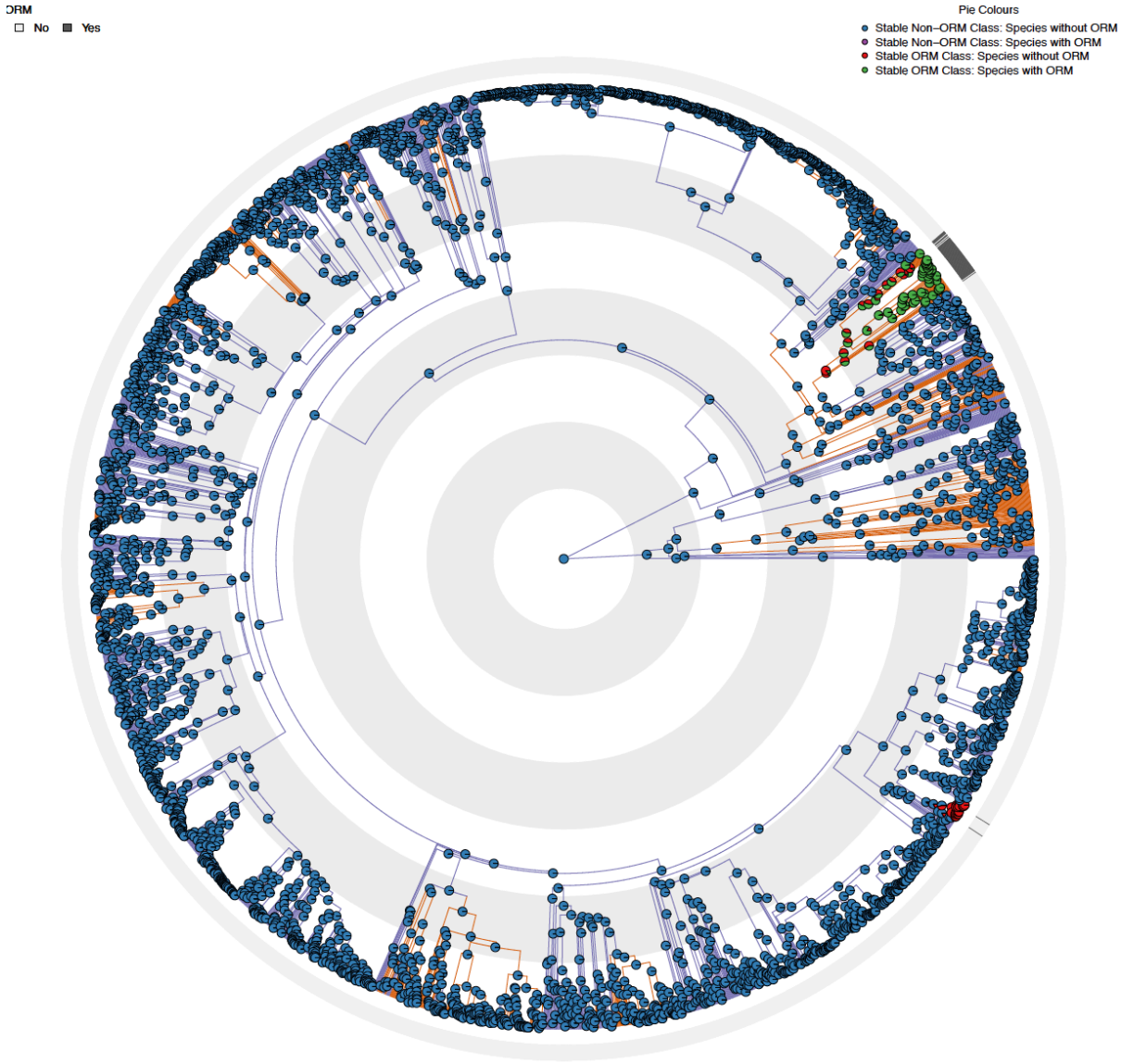

SI Figure 4: The pie charts in this figure depict the ancestral state reconstruction of plant-orchid fungi (ORM) interactions under the best HRM-model (SI Table 1). The coloured band across the phylogeny indicate the reported presence (dark grey) or absence of ORM interactions across our 3,736 species. The branch colours indicate the reconstructed presence (purple) or absence (orange) of AM fungi under the best HRM-model for plant-AM interactions (Table 1, SI Figures 1 & 2). We visually observe that AM-loss co-occurs with a shift to ORM fungi in the Orchids.

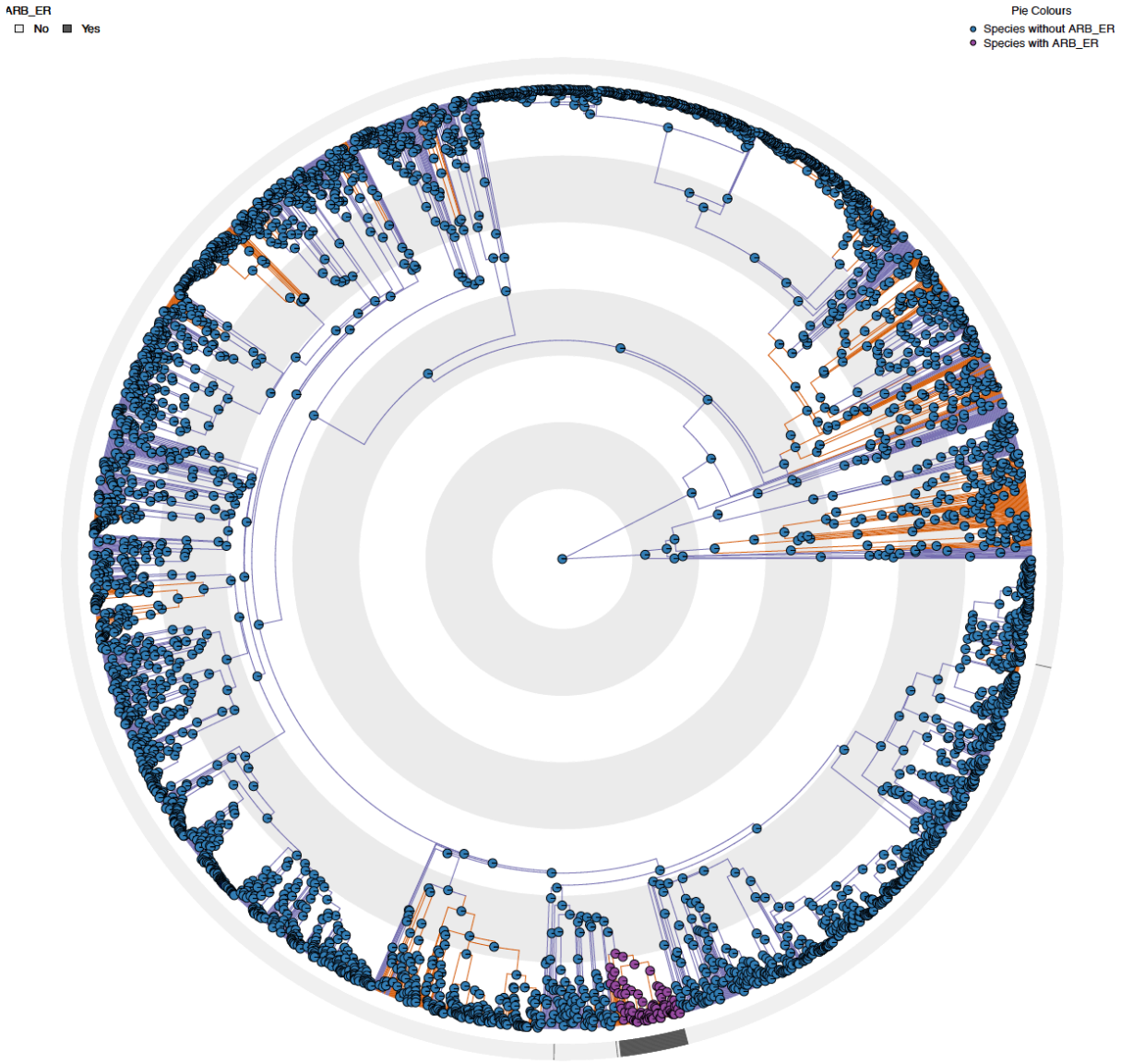

SI Figure 5: The pie charts in this figure depict the ancestral state reconstruction of plant interactions with either Arbutoid (ARB) and Ericoid (ER) mycorrhizal fungi under the best HRM-model (SI Table 1). The coloured band across the phylogeny indicate the reported presence (dark grey) or absence of ARB or ER interactions across our 3,736 species. The branch colours indicate the reconstructed presence (purple) or absence (orange) of AM fungi under the best HRM-model for plant-AM interactions (Table 1, SI Figures 1 & 2). We visually observe that the evolution of the ARB/ER interactions co-occurs with the loss of AM interactions in the Ericales.

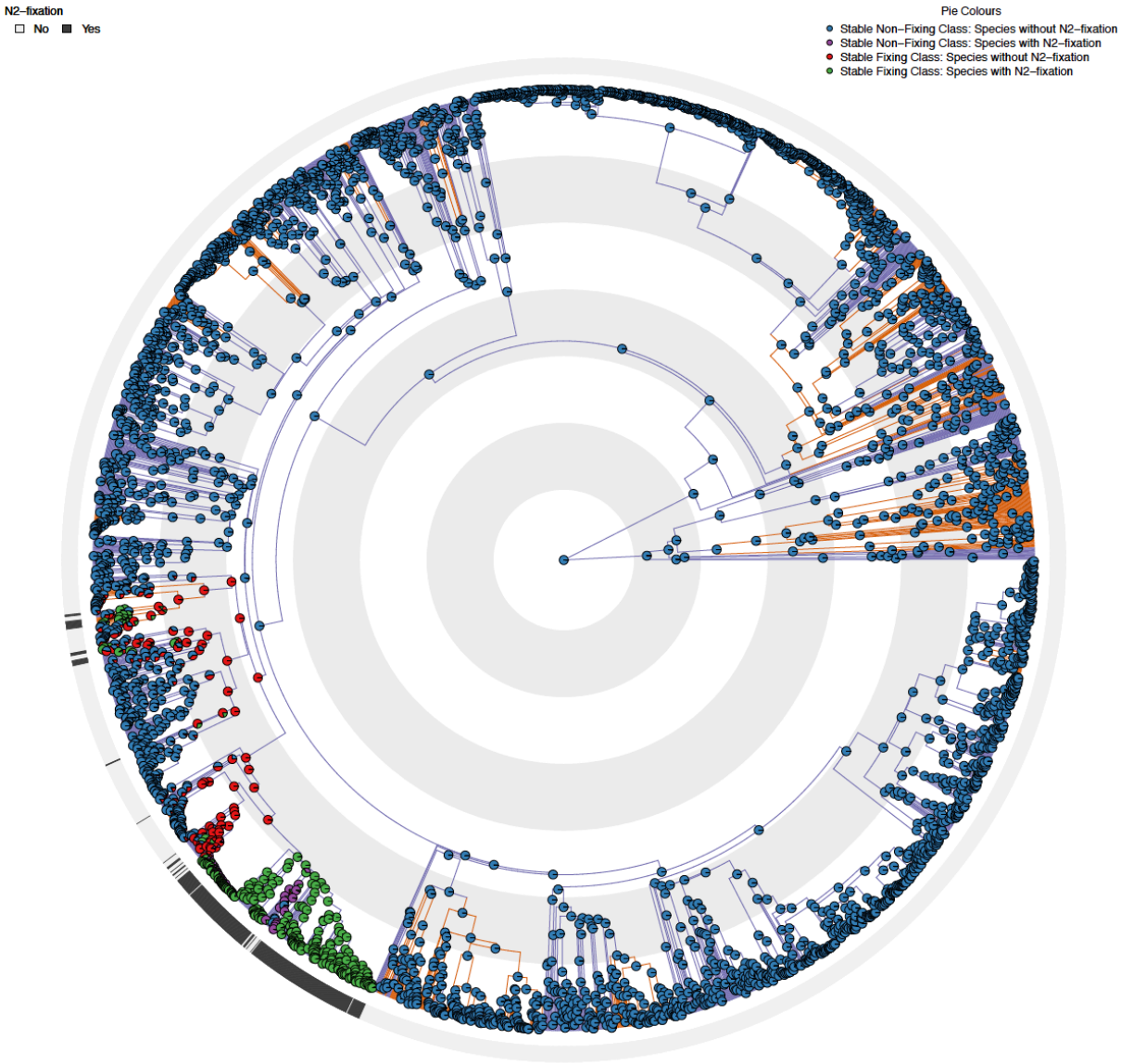

SI Figure 6: The pie charts in this figure depict the ancestral state reconstruction of plant interactions with symbiotic N2-fixation under the best HRM-model (SI Table 1). The coloured band across the phylogeny indicate the reported presence (dark grey) or absence of nodulation across our 3,736 species. The branch colours indicate the reconstructed presence (purple) or absence (orange) of AM fungi under the best HRM-model for plant-AM interactions (Table 1, SI Figures 1 & 2). We visually observe that the evolution of symbiotic N_2-fixation is unconnected with the loss of AM interactions in the Fabaceae, but co-occurs among some of the Fagales.

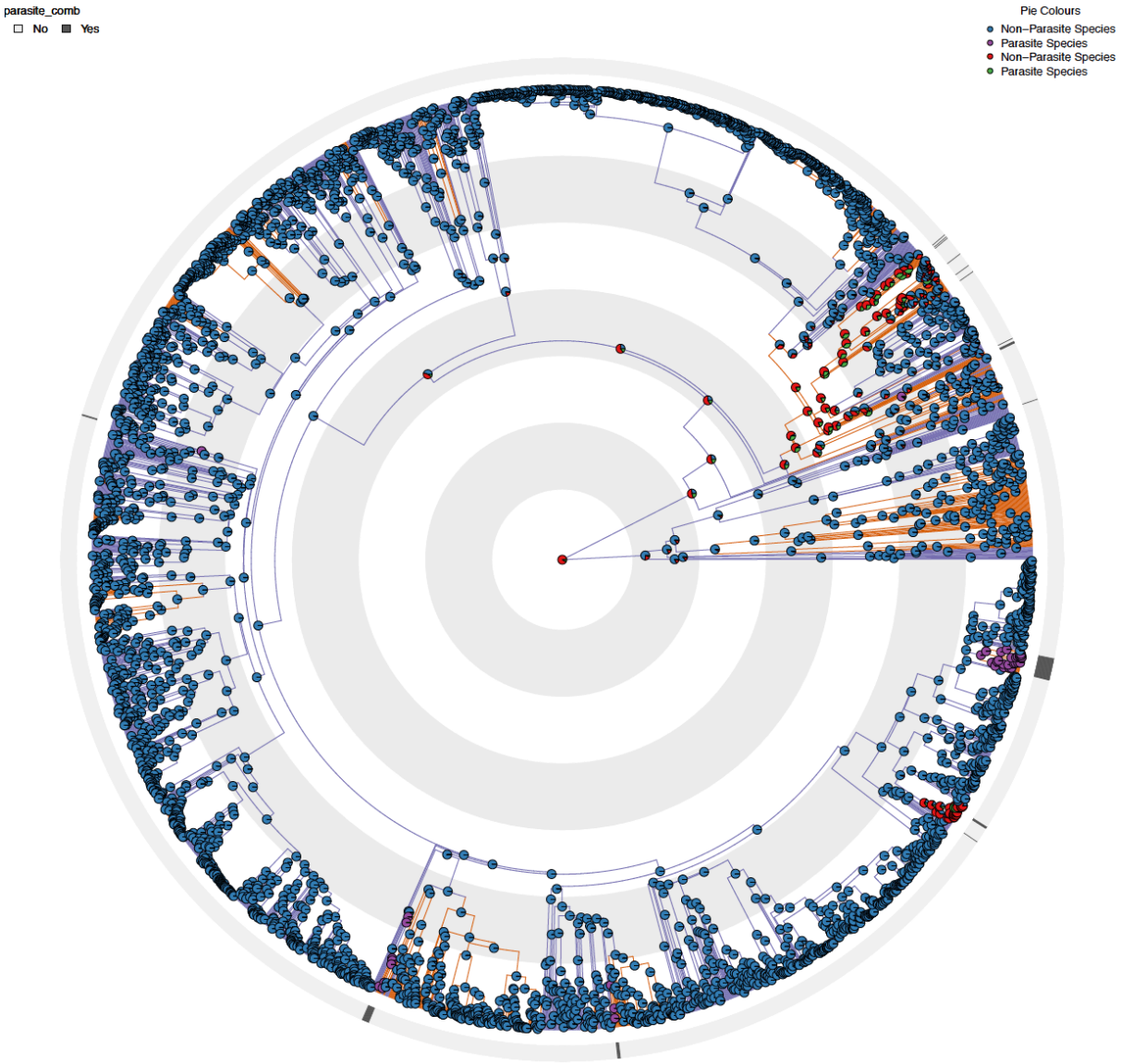

SI Figure 7: The pie charts in this figure depict the ancestral state reconstruction of plant parasitism under the best HRM-model (SI Table 1). The coloured band across the phylogeny indicate the reported presence (dark grey) or absence of plant parasitism across our 3,736 species (i.e. the data that the reconstruction indicated by the pie charts is based on). The branch colours indicate the reconstructed presence (purple) or absence (orange) of AM fungi under the best HRM-model for plant-AM interactions (Table 1, SI Figures 1 & 2). We observe that, visually, AM-loss co-occurs with a shift to plant parasitism in four clades.

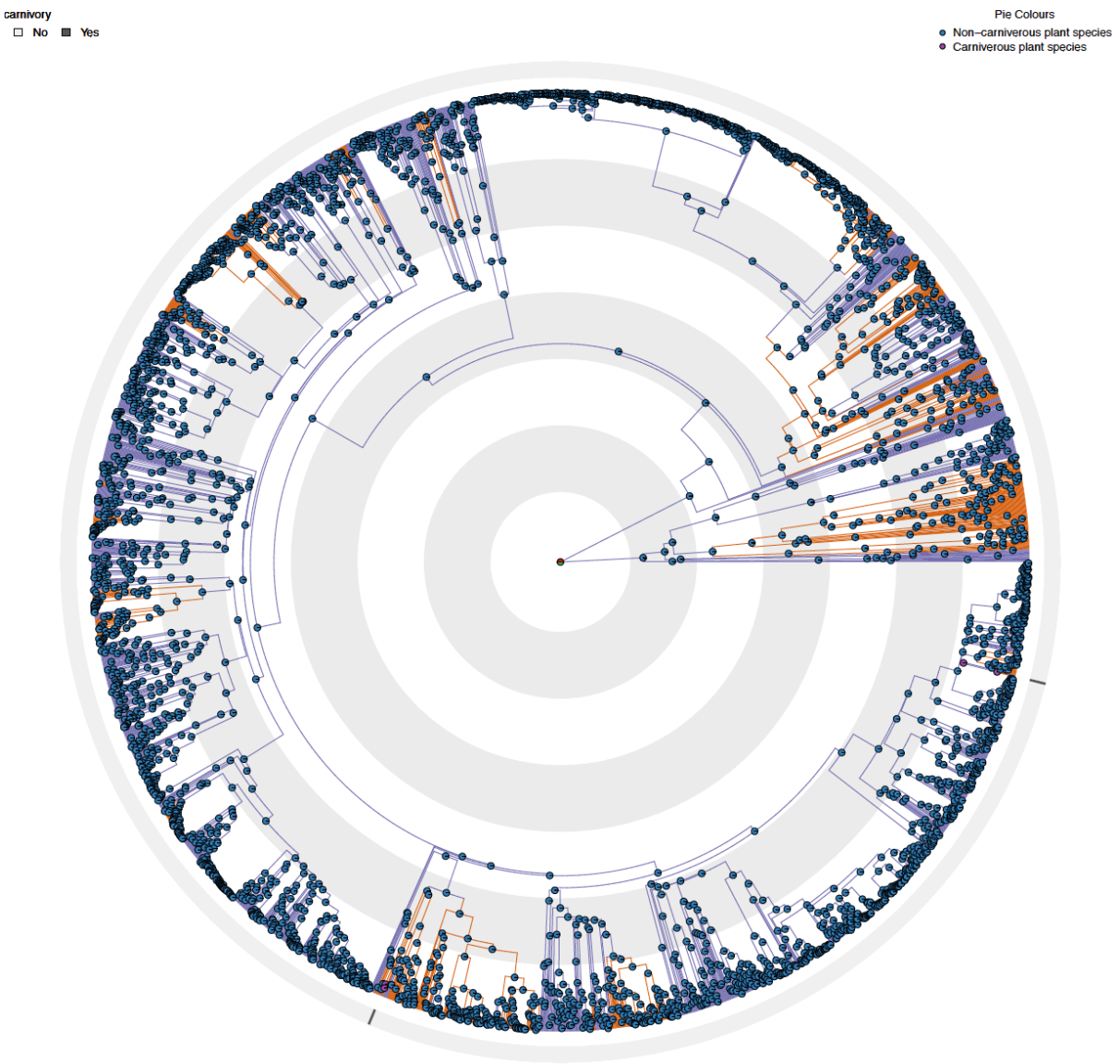

SI Figure 8: The pie charts in this figure depict the ancestral state reconstruction of plant carnivory under the best HRM-model (SI Table 1). The coloured band across the phylogeny indicate the reported presence (dark grey) or absence of carnivory across our 3,736 species (i.e. the data that the reconstruction indicated by the pie charts is based on). The branch colours indicate the reconstructed presence (purple) or absence (orange) of AM fungi under the best HRM-model for plant-AM interactions (Table 1, SI Figures 1 & 2). We observe that, visually, AM-loss co-occurs with a shift to plant carnivory in two clades.

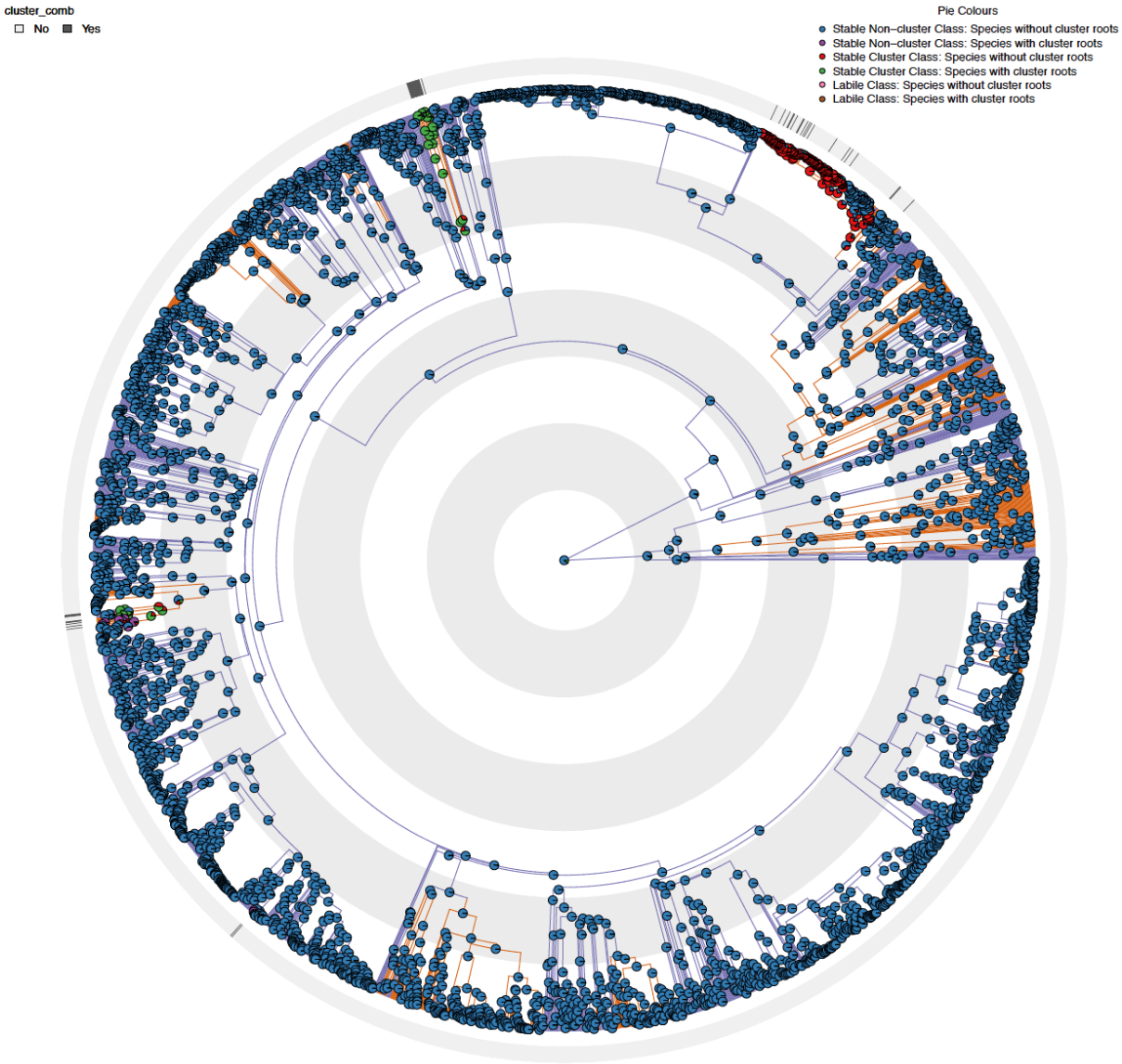

SI Figure 9: The pie charts in this figure depict the ancestral state reconstruction of cluster roots under the best HRM-model (SI Table 1). The coloured band across the phylogeny indicate the reported presence (dark grey) or absence of cluster roots across our 3,736 species (i.e. the data that the reconstruction indicated by the pie charts is based on). The branch colours indicate the reconstructed presence (purple) or absence (orange) of AM fungi under the best HRM-model for plant-AM interactions (Table 1, SI Figures 1 & 2). We observe that, visually, AM-loss co-occurs with a shift to cluster roots in three clades.

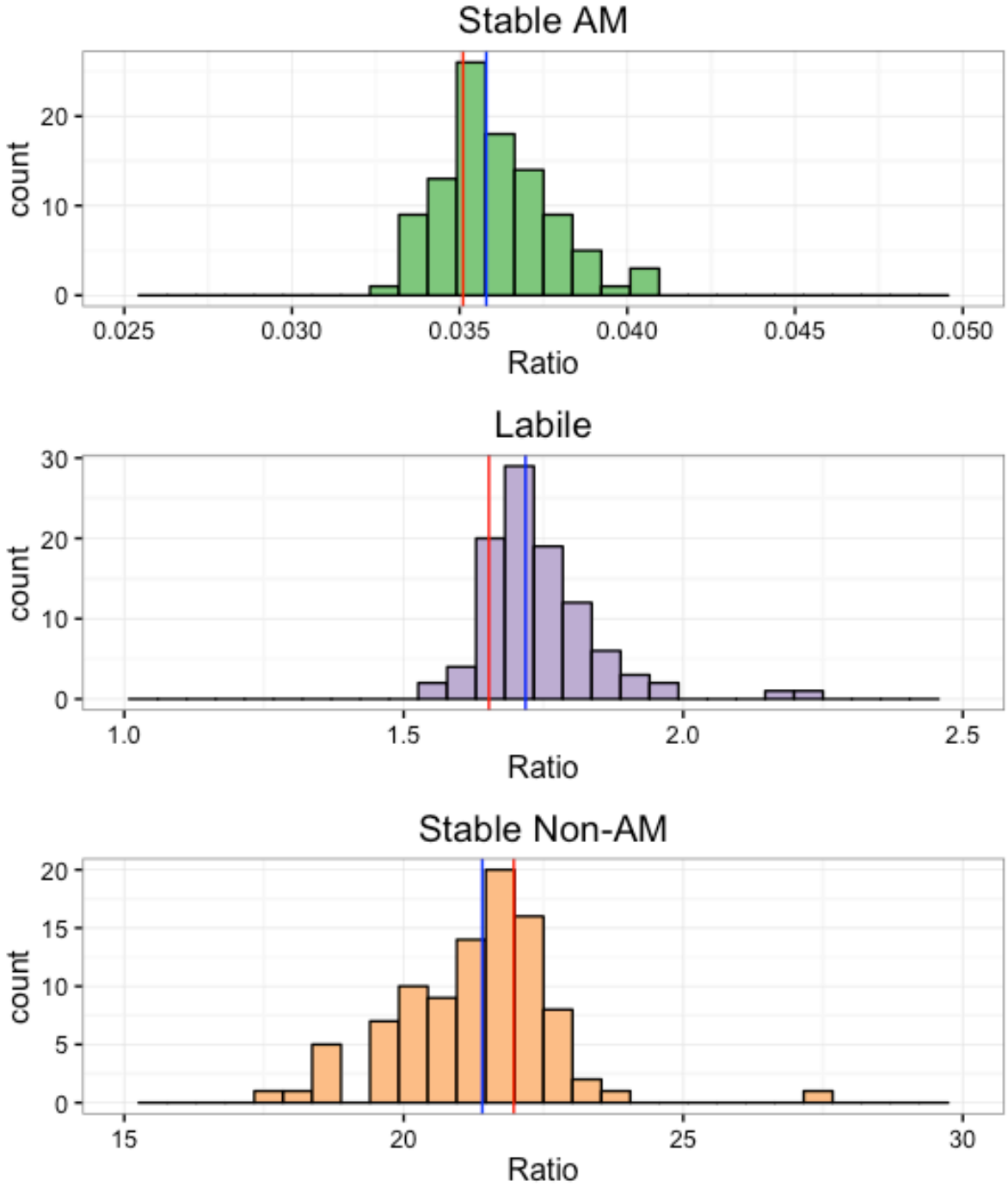

SI Figure 10: *We reran our three rate class HRM on hundred bootstrap phylogenies* (1)*, and similarly determined the ratio of AM loss to AM gain (AM_{loss}/AM_{gain}) as in SI Figure 1. This ratio within the three hidden rate classes is printed above (colour is the same as in SI Figures 1 and 2). We found that throughout these hundred reruns, independent of phylogeny considered, the relative loss and gain rate in the three main stability classes were highly stable. This is indicated by the similar median values over hundred reruns (blue line) compared to the ratio under the 'best' phylogeny (red line), by the close clustering of all values around this 'best' estimate, and by the non-overlapping distributions.*

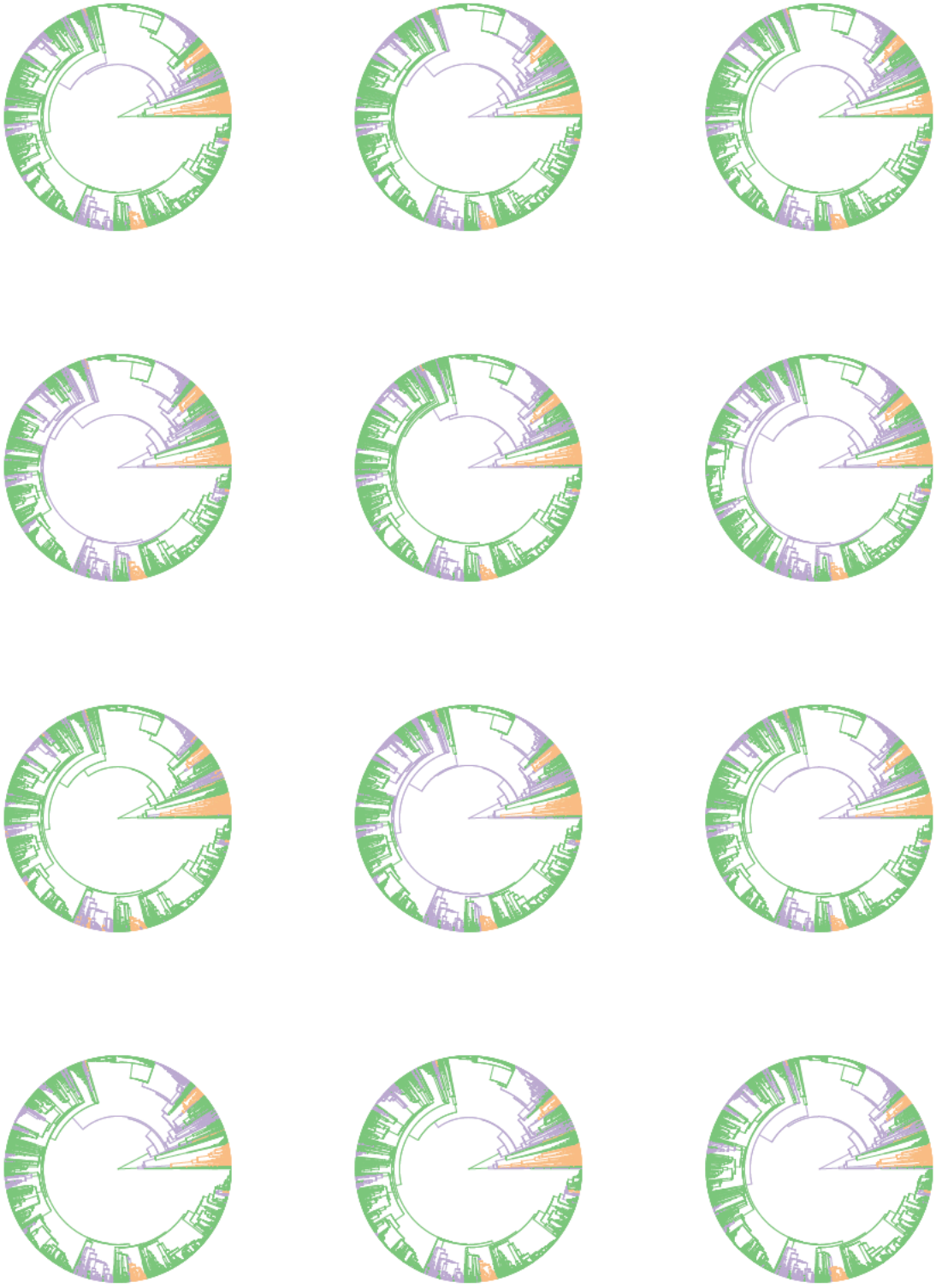

SI Figure 11: We reran our three rate class HRM on hundred bootstrap phylogenies(1)***, and similarly to previously, printed the three AMF stability classes on the phylogenies. The top left phylogeny represents the reconstruction under the 'best' phylogeny, i.e. the same figure as SI Figure 2 (leaving out the pie charts for visual clarity). The other 11 phylogenies represent randomly selected phylogenies from among the 100 bootstrap phylogenies. We observe very similar patterns of evolution of the stable AM state (green), the labile state (purple) and the stable AM loss (orange) throughout.***

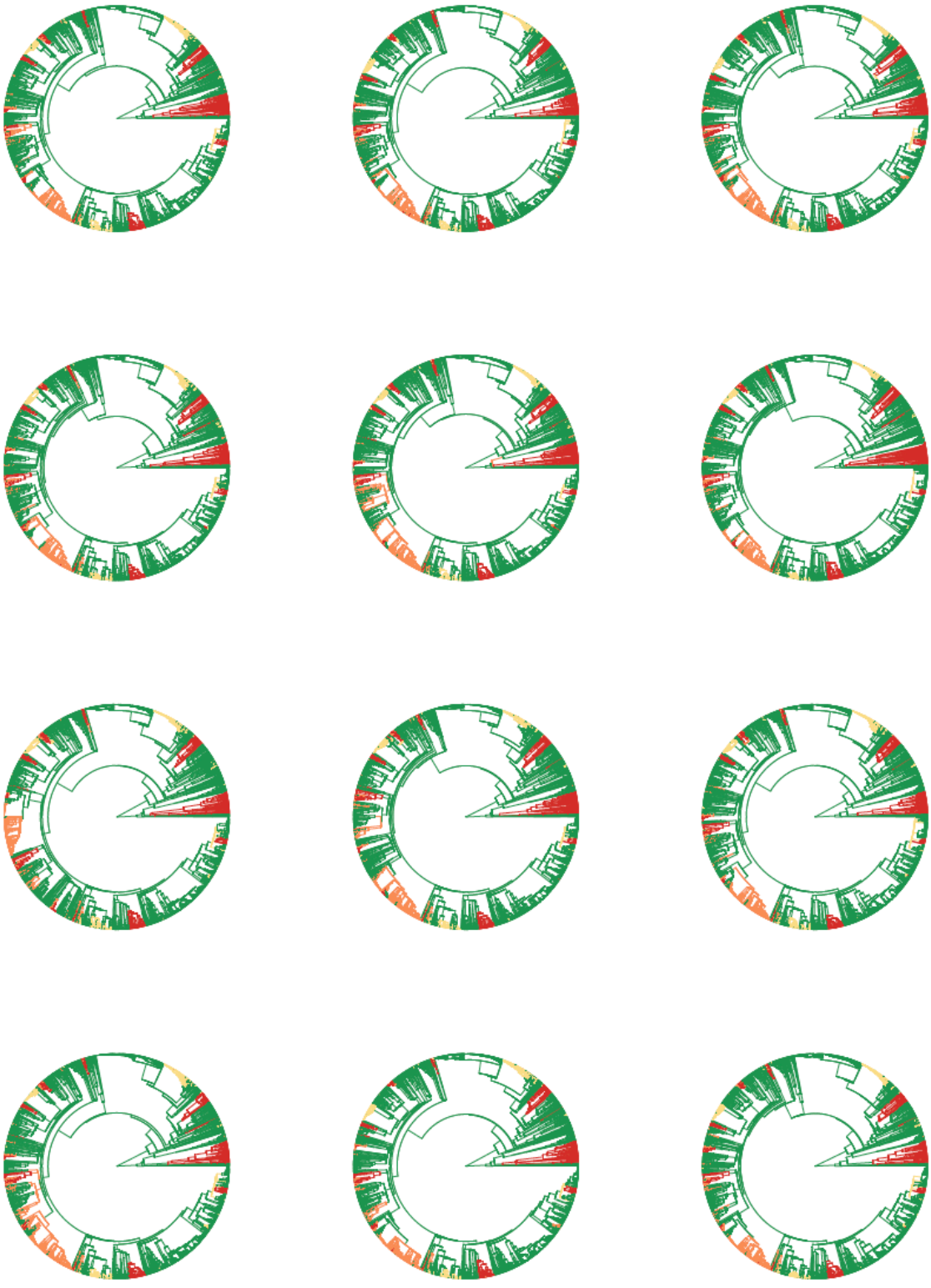

SI Figure 12: We reran our dependent model of AM and AM-alternative evolution (Figure 2) on hundred bootstrap phylogenies(1) ***and printed the four states under the reconstruction on the phylogenies. The top left phylogeny represents the reconstruction under the 'best' phylogeny, i.e. the same as in Figure 2 (leaving out the circular bands for visual clarity). As previously, the other 11 phylogenies represent randomly selected phylogenies from among the 100 bootstrap phylogenies. We observe very similar patterns of evolution regardless of the precise phylogeny used.***

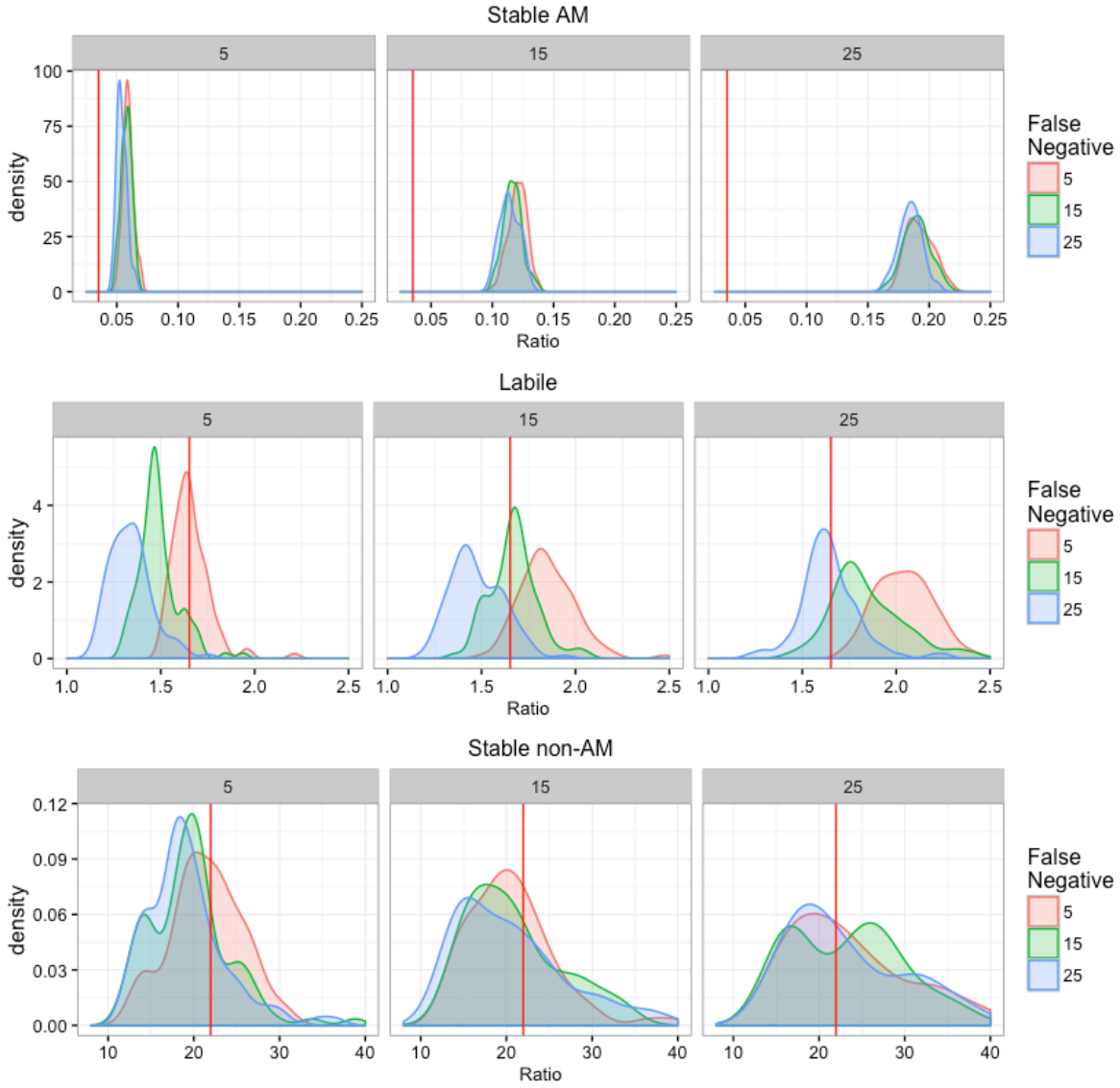

SI Figure 13: We resimulated our main AM dataset assuming both false negative and false positive rates of 5%, 15% and 25%, or a total of nine potential combinations (or conversely $P_{correct}$ equals 0.95, 0.85 or 0.75; see Methods). Each combination was resimulated a hundred times. The AM loss to AM gain ratios (AM_{loss}/AM_{gain}) for the resulting three rate class HRMs are shown in this Figure, red lines indicate the estimate in the default model assuming all data are accurate (i.e. the rates from SI Figure 1). The three columns indicate false positive rates of 5, 15 and 25%, the three rows indicate the three AM stability classes and the three overlapping coloured density distributions indicate false negative percentages of 5% (red), 15% (green) and 25% (blue). Higher false positive percentages mean that the number of AM presence reports in the original data has been overestimated, so resimulating under this assumption results in fewer AM species, increasing relative loss rates and shifting the distribution to the right. Thus, we expect distributions to shift to the right more in the right column than in the left. In contrast, higher false negative percentages (blue) have the opposite effect and are expected to shift the distribution to the left. These are indeed the effects we observe, particularly for the stable AM and the intermediate classes. In general, this figure indicates that even with 25% false positive rates and 25% false negative rates (blue density curve in the right column), i.e. if we assume that the field is very bad in accurately detecting AM fungi in plants and generates both a lot of false positives and a lot of false negatives, the three rate classes are still very robust and highly different. This means that our conclusion of three distinct stability classes (SI Figures 1 & 2) is robust to even very high levels of inaccuracy in our underlying data.

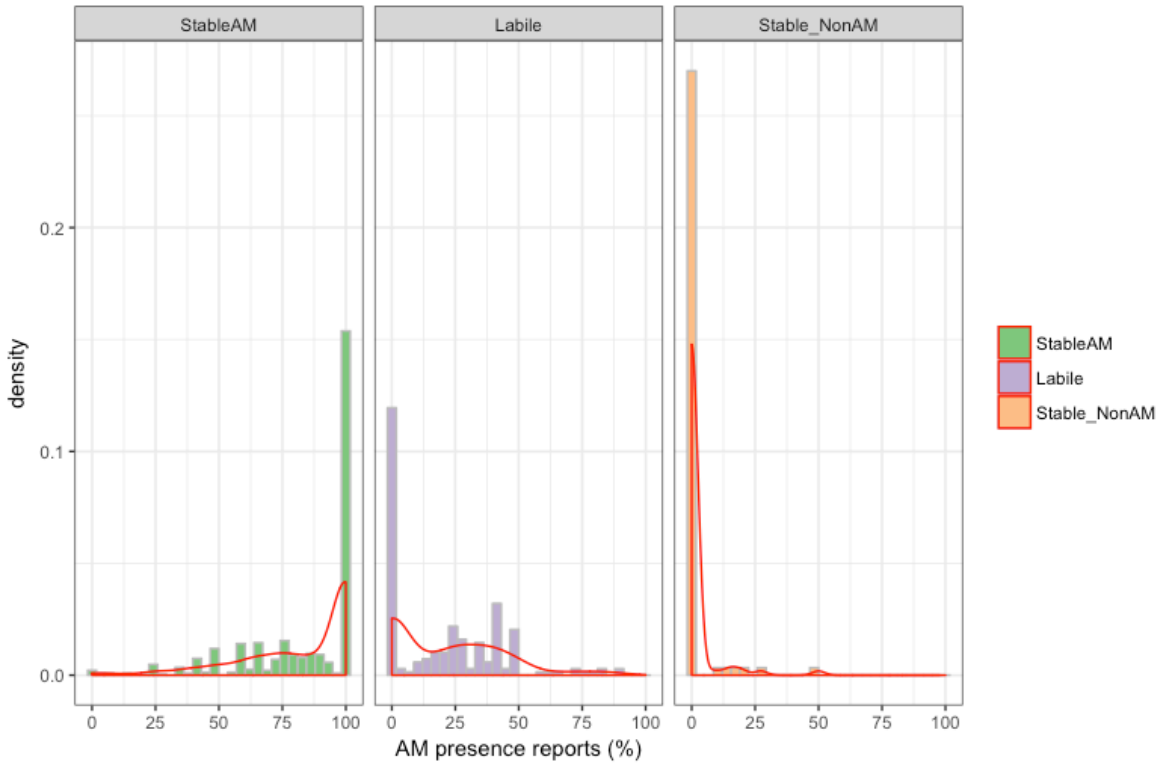

SI Figure 14. Histogram of the percentages of observations that was with a AM-interaction present, by evolutionary state as inferred under our best three-rate class HRM-model (Table 1, SI Figure 1). As expected, we find that for the stable AM class and particularly the stable Non-AM class are predominantly either always mycorrhizal, or never. In contrast, in the labile class, while many species are non-mycorrhizal across all observations, there is a large group of species with both AM and presence reports, resulting in a median value of 0.167 for proportion of AM presence observations. This figure only includes species with more than three observations per species, because all singleton species with a single observation by definition are uniformly (non-)mycorrhizal. Releasing this constraint results in a qualitatively highly similar figure (not shown).

SI Table 1: Best ancestral state reconstruction (HRM-model) for AM-alternatives

AM Alternative	Best HRM-model	AICc-weight
Other root symbionts		
Ectomycorrhizal (ECM)	3 rate classes	51.6%
Orchid mycorrhizal (ORM)	2 rate classes	87.2%
Ericoid & Arbutoid (ER & ARB)	1 rate class	99.4%
Symbiotic N_2-fixation	2 rate classes	97.7%
Alternative resource strategies		
Plant parasitism	2 rate classes	95.7%
Carnivory	1 rate class	99.7%
Cluster Roots	3 rate classes	99.2%

For each of the considered AM alternatives (both other root symbionts and alternative resource acquisition strategies), we created HRM models assuming 1 to 5 different rate classes. This table presents the best (as determined by AICc-weights) model among this set of five candidate models. We present the corresponding ancestral state reconstruction above in SI Figures 3 – 9.

SI Table 2: Mean Δ-AICc across 100 replicates of different resimulated false positive and false negative rates.

False positive rate	False negative rate	Mean Δ-AICc
5%	5%	388.4
5%	15%	412.7
5%	25%	440.6
15%	5%	376.8
15%	15%	399.9
15%	25%	417.8
25%	5%	340.6
25%	15%	357.4
25%	25%	381.2

Using the same re-simulated AM datasets from SI Figure 13, we analysed both dependent and independent models of AM and AM alternative evolution (see Methods). We report the mean Δ-AICc between independent and dependent models of evolution (positive values indicate a better fit of the dependent model), and find that the dependent model outperformed the independent one in all resimulations.

Extended Methods

Mycorrhizal status database

We compiled our database of reported plant mycorrhizal status by obtaining data through: (i) the TRY plant trait initiative (2) (from data sources (3, 4)), (ii) a recently digitised database from the former Soviet Union (5), (iii) the MycoFlor database of plant mycorrhizal status (6), (iv) digitising a review of plant mycorrhizal status (7) and (v) further supplementing these with manual literature searches (8–30). We first checked all plant species names, and then resolved inaccuracies, using the Taxonomic Name Resolution service v4.0(31) and if necessary verified these manually using The Plant List (32). Records that were not characterised to species level were excluded.

We combined these sources to compile a single database of reported plant mycorrhizal status. We included reports for interactions with arbuscular mycorrhizal (AM) fungi, and a number of rarer mycorrhizal fungi: ectomycorrhizal fungi (EM), orchid mycorrhizal (ORM), Arbutoid (ARB) and ericoid mycorrhizal (ER) fungi (33) and we also scored non-mycorrhizal reports (i.e. plants reported to not interact with mycorrhizae). We tallied the number of observations for each of these states per species present across the databases. We were interested in the evolution of the capacity of plant species to engage in mutualism with AM fungi, and therefore we assigned all those species present in our database for which there was at least one reported observation of an AM (or respectively ECM, ER etc.) interaction as a "Yes". Since AM fungal interactions are plastic and plants capable of forming an AM fungal symbiosis do not do so under all conditions, this can result in species with a single or few observations being assigned a 'No', while they are in principle capable of forming an AM fungal symbiosis. Ideally, we would directly observe the underlying fundamental capacity (or incapacity) for AM interactions, but this is unobservable at a large scale. We therefore followed this coding scheme, and studied the sensitivity of our conclusions to uncertainty in data assignment, including high simulated rates of false negative reports (see '*Sensitivity Analysis to Uncertainty in the Data'*).

Following this procedure, we obtained the mycorrhizal status for a total of 9,715 species (based on a total of 22,394 observations, *i.e.* 3.09 per species). Of these there were 3,736 spermatophyte species (3,530 angiosperms, 206 gymnosperms) that overlapped with the phylogeny used in our analysis (34). In this analysed dataset, there were a total of 14,383 observations (mean number of observations per species: 3.85). We have made our analysed database available online, including the number of reports per category per species (Supporting Data 1).

Spermatophyte phylogeny

We used the spermatophyte phylogeny generated by Zanne et al. (1, 34), as it is currently the largest and most comprehensive phylogeny of global land plants, containing a total of 32,223 species. We pruned the phylogeny to the overlap of 3,736 species with our mycorrhizal database, retaining 61 orders, 230 families and 1,629 genera in total. This covers a wide diversity of plant life and evolutionary history (a cumulative 70.7 billion lineage years of evolution is represented in the pruned phylogeny).

Phylogenetic Reconstruction of the evolution of AM interactions

Our aim was to first determine the evolutionary history of the AM fungal symbiosis, and identify when and where the partnership was lost. Since we were analysing evolutionary processes over thousands of clades going back 352 million years (the estimated age of the last common ancestor of spermatophytes in our phylogeny), we expected heterogeneity in the speed of evolution of plant-AM interactions. Therefore, we used a Hidden Markov Model approach to binary character state evolution called 'Hidden Rate Models' (HRMs) (35). This method allows for heterogeneity in the loss and gain rates of a binary trait across a phylogeny (in this case reported AM presence vs. absence, see *Mycorrhizal database*), allowing us to better reconstruct the evolutionary history of the plant-AM interactions, including potential evolutionary breakdowns.

We used the R-package *corHMM* (35) (version 1.18) in R 3.2.3 to analyse our mycorrhizal data and explored HRMs with one to five rate classes. To prevent model overfitting, we used AICc-weights (36) to select the best HRM among this family of candidate models (Table 1). We found that by far the best model was a model with three rate classes and further analysed the associated transition rate matrix and ancestral state reconstructions. We used the marginal method to perform ancestral state reconstructions and employed Yang's method to use the estimated transition rates to compute the root state (37). This means that we did not fix root states in our reconstructions, and can also use our analysis to determine the most likely ancestral AM state of spermatophytes. We concluded that the likely ancestral state of spermatophytes was AM fungal association, which is in agreement with the fossil record (38–40), with a recent phylogenetic reconstruction of mycorrhizal states in land plants (41) and with recent phylogenomic work (42, 43).

To facilitate model interpretation, we multiplied transition rates by 100 expressing them in number of transitions per 100 million years (SI Figure 1). We observed that the three rate classes assumed under the best model corresponded to a class where AM are strongly favoured, an intermediate labile class and a class where a non-AM character state is strongly favoured over evolutionary time. Consequentially, we *a posteriori* called these classes 'Stable AM', 'Labile' and 'Stable Non-AM' (SI Figure 1). This biological pattern is not an inherent constraint of the model analysed, since we allowed for all rates to vary freely, but rather the most likely rate matrix based on our phylogeny and data. For

each species analysed, we provided the likelihoods of inferred rate classes (Stable AM, Labile, Stable Non-AM), as well as the likelihood of AM interactions being retained in supporting online data (Supporting Data 1).

Number of AM Losses

In order to calculate the number of evolutionary losses of the AM state across the phylogeny under our best evolutionary model (Table 1, SI Figure 1), we used the multinomial probabilities calculated for each node in our ancestral state reconstruction. We followed an approach previously developed (44), where we sum the appropriate differences in state probability among nodes across the full phylogeny for each transition of interest. Under a maximum parsimony assumption, this summation corresponds to the expected number of events that has occurred across the entire phylogeny. We used a cut-off of 1% between two nodes to exclude small fluctuations that do not represent evolutionary transitions but uncertainty in the method, and found a total of 24.6 AM losses. We repeated this approach across the 100 bootstrap angiosperm phylogenies we analysed (see *Phylogenetic Uncertainty*) to obtain a median value and SD for the number of AM losses. These calculations refer to the number of evolutionarily stable breakdowns of plant-AM interactions. The number of breakdowns followed by extinction of the plant host is not detected in our analyses and may be higher.

Database Alternative Resource Acquisition Strategies

In order to test for relationships among plant AM-losses and the evolution of alternative resource strategies, we generated two further databases. First, we scored all our 3,736 species for three main alternative resource strategies: carnivory, parasitism and cluster roots. Each of these strategies represents an alternative way of extracting minerals from the environment: carnivory from animal sources particularly insects (45, 46), parasitising either other plants (47, 48) or from mycorrhizal fungi (49) (*i.e.* also obtaining (all) carbon from the parasitised fungus or plant) and cluster roots by forming an extensive and finely branched network of fine roots (50, 51). To score plant species for carnivory status we used the Carnivorous Plants Database (52), supplemented with information from primary literature (45, 53, 54). For parasitism, we used information from the Parasitic Plants Database (55) and the primary literature (47–49, 56). We included both hemiparasites and holoparasites, because both obtain mineral nutrients (and water) from other plants, but not epiphytes because these generally only obtain structural support from their host plants. We also included plants parasitising mycorrhizal fungi (mycoheterotrophs), but not mixotroph plants that both parasitise mycorrhizal fungi and independently acquire nutrients (57). To score our phylogeny species for cluster roots we used information from the primary literature (50, 51, 58, 59). In cluster roots we also include dauciform roots, a type of roots that is structurally different but functionally analogous to true cluster roots (60).

Second, we included in our database the presence or absence of symbiotic nitrogen-fixation, both through rhizobial as well as with *Frankia* bacteria (61). We used our previously generated database on symbiotic nitrogen-fixation status to assign nitrogen-fixation status to all our species analysed here (44, 62). For all our assignments, we were conservative in assigning a species for carnivory, parasitism, cluster or symbiotic nitrogen-fixation status: we only did so if we had a positive indication that it, or a closely related species or genus, could be characterised as such, and that there was no variation in character state at that taxonomic level. Consequentially, we have potentially missed a number of parasites, carnivorous plants and cluster roots. This is particularly likely to be the case for cluster roots. These have been described in the sedges (*Carex*) (63), for which we have 110 species in our analysis. Yet, not all *Carex* have cluster roots and consequentially we have only scored those for which we have a positive report as forming cluster roots. In general, since we are interested in calculating the relation between AM-loss and the evolution of alternative strategies, this strategy is likely to underestimate the strength of this correlation making our analysis more conservative.

Correlated evolution of AM interactions and AM-alternatives

Having compiled databases for non-AM mycorrhizal fungi and adaptations for resource acquisition, we generated HRM-models (35) (SI Table 1) for three other mycorrhizal fungi (EM, ORM and ER/ARB fungi), for symbiotic nitrogen-fixation, as well as for three alternative resource strategies (carnivory, parasitism and cluster roots) and reconstructed their ancestral states as previously for AM interactions (see: *Phylogenetic Reconstruction of the evolution of AM interactions*). We visually identified the origins of these AM-alternatives and plotted them onto our AM ancestral state reconstruction (SI Figure 3-9). We then tested the potential for correlated evolution among AM fungi, other mycorrhizal fungi and resource acquisition adaptations. We compared models of dependent and independent evolution (64, 65) among the binary variables AM (presence/absence) and AM-alternatives (*i.e.* a binary variable coding for the presence of any other mycorrhizal fungus, symbiotic-nitrogen fixation or alternative resource acquisition strategy). This allowed us to determine if AM interactions evolved independently from AM alternatives. We used the Maximum Likelihood implementation of the Discrete-module in *BayesTraits V2*, and constrained the ancestral node of our seed plant phylogeny to have AM fungi but none of the alternatives, as that is what our previous analyses had revealed (SI Figures 2-9). Using AICc-values, we found that the dependent model of evolution, which assumes the evolution of both variables and in which the character state of one variable depends on the character state value for the other variable, vastly outperformed an independent model. We therefore selected this dependent evolution model. We used the transition rates to reconstruct the four potential ancestral states across our phylogeny (Figure 2), using the *corDISC* function in the R-package *corHMM* (35). In order to further analyse this model, we again multiplied transition rates to express them in transitions per 100 million years. We used the R-package *diversitree* (0.9-8) to plot the reconstruction of the four potential

states onto our seed plant phylogeny and plot the raw explanatory AM, other MF and alternative resource acquisition strategies as circular bands around the phylogeny (66) (Figure 2).

Sensitivity analysis to phylogenetic uncertainty

The phylogeny is a source of uncertainty in any comparative study. In order to address this, we regenerated our three rate class HRM-model, the best model for AM-evolution (Table 1) across 100 bootstrap phylogenies (1). This allows us to study if our three stability classes are robust across many potential other topologies and branch lengths of the spermatophyte phylogeny. We find that across the 100 bootstrap phylogenies, the three stability classes are robust in all cases, and that the relative evolutionary stability (AM_{loss}/AM_{gain}) of AM is replicated throughout (SI Figure 10). We also find highly similar ancestral state reconstruction of potential evolutionary states across all 100 phylogenies (SI Figure 11). This further reinforces our interpretation that the three stability classes are highly robust to phylogenetic uncertainty. We repeated our dependent and independent evolutionary models of AM and AM-alternative evolution across these same 100 bootstrap phylogenies. This revealed that across 100% of the phylogenies, the dependent model of evolution vastly outperformed the independent model (mean Δ-AICc in favour of the dependent model: 525.40, minimum Δ-AICc 428.57). Here too, the ancestral state reconstructions are virtually identical across the 100 phylogenies (SI Figure 12). Thus, we conclude that both our primary AM reconstruction and our key results of dependent evolution among AM loss and AM-alternatives, is highly robust to phylogenetic uncertainty.

Sensitivity analysis to uncertainty in the data

Both the absence of AM fungi in a root system (false negative), as well as its presence can be misinterpreted (false positive). This is particularly important since the visual scoring techniques that were historically employed to score AM fungi in plant roots, and upon which most of the observations in our database are based, are sensitive to misinterpretation in both directions. We were therefore needed to test if low data quality and potential bias in our database would distort our results. For instance, in the Brassicales, where widespread loss of the genes mediating AM interactions has been reported (43, 67), a few of the AM presences reported are likely erroneous. Removing these data points from analysis before performing ancestral state reconstructions and other comparative analysis, would be circular since it could lead us to conclude that some clades show increased loss rates precisely because we had removed presence reports based on an implicit phylogenetic criterion (*e.g.* on the assumption that Brassicales AM presence reports are more likely to be erroneous). Therefore, in order to address the potential concern of low AM fungal data quality, we employed a resimulation technique and regenerated our database many times under different assumptions for rates of false positive and false negative rates. This allows us to separately model scenarios where the scientific field as a whole is very poor at detecting AM fungi that are actually there (high false negatives) or very likely to detect AM fungi when none are there (high false positives), or both.

Essentially, each observation of AM presence or absence a scientist makes represents a Bernoulli trial with a given (and unknown) likelihood $P_{correct}$ of the researcher correctly observing the true underlying character state (which is unknowable). Thus, we place more trust in a species' capacity to interact with AM if there are more observations of it doing so, since it becomes less likely these observations are all wrong. Since we tallied the number of AM presence (and absence) reports (N_{AM} and N_{NM}) for all our species (see *Mycorrhizal Database*) we could use this logic to resimulate our observations using this number and a range of values for $P_{correct}$. Thus, for each species, observations where resimulated as a Bernoulli trial $B(N_{AM},P_{correct})$. Then, we assigned the species a new, potentially changed AM state as previously (*i.e.* 'Yes' if at least one positive resimulated report remained, as under the original coding scheme). We repeated this both for AM presence and absence reports, to simulate both false positive and false negative character assignment of the original research data. Both for false positive and for false negatives, we used $P_{correct}$ likelihoods of 0.75, 0.85 and 0.95, thus giving a total of nine (3*3) combinations. For instance, $P_{correct} = 0.75$ indicates that a researcher has only a 75% chance of correctly observing the right AM state.

This procedure allowed us to study both the effect of high false positive percentages (up to 25%), i.e. a field that is likely to over report AM, and high false negative percentages, i.e. a field that is likely to miss many AM, as well as combinations of these (e.g. high false positive, low false negative). We resimulated each of our nine combinations of false positive and negative percentages 100 times, creating 900 resimulated databases. As previously, we regenerated our three-rate class HRM model for all of these, and analysed relative transition rates (AM_{loss}/AM_{gain}) in all stability classes (SI Figure 13). While we found, as expected, that an assumption of high false positive rates increases relative loss rates inferred in the HRM model (and the converse for high false negative rates), the key conclusion of this analysis is that the three stability classes are highly robust even to high false negative and false positive rates simultaneously (i.e. to a field which is both very bad at detecting AM and at scoring non-mycorrhizal plants). This is shown by the fact that regardless of the precise $P_{correct}$ used, AM_{loss}/AM_{gain}-ratios cluster close to the estimate under the best model and form clearly distinct, non-overlapping categories (SI Figure 13). We visually analysed the ancestral state reconstructions of these 900 resimulated models and found the patterns to be in general agreement with those under our best model, even for low values of $P_{correct}$. Lastly, for the same resimulated datasets we analysed the relative performance of a dependent model versus an independent model of AM and AM-alternative evolution. We found that throughout our resimulations, even for the lowest values of $P_{correct}$, the dependent model always outperformed the independent one (SI Table 2). These analyses confirm that our main conclusions are robust to even very high levels of inaccuracy in our underlying data.

Supporting Information References

1. Zanne AE, et al. (2013) Data from: Three keys to the radiation of angiosperms into freezing environments. *Dryad Digit Repos*. doi:10.5061/dryad.63q27/3.
2. Kattge J, et al. (2011) TRY - a global database of plant traits. *Glob Chang Biol* 17(9):2905–2935.
3. Craine JM, et al. (2009) Global patterns of foliar nitrogen isotopes and their relationships with climate, mycorrhizal fungi, foliar nutrient concentrations, and nitrogen availability. *New Phytol* 183(4):980–92.
4. Cornelissen JHC, Aerts R, Cerabolini B, Werger MJA, van der Heijden MGA (2001) Carbon cycling traits of plant species are linked with mycorrhizal strategy. *Oecologia* 129(4):611–9.
5. Akhmetzhanova AA, et al. (2012) A rediscovered treasure: mycorrhizal intensity database for 3000 vascular plant species across the former Soviet Union. *Ecology* 93(3):689–690.
6. Hempel S, et al. (2013) Mycorrhizas in the Central European flora: relationships with plant life history traits and ecology. *Ecology* 94(6):1389–99.
7. Wang B, Qiu Y-L (2006) Phylogenetic distribution and evolution of mycorrhizas in land plants. *Mycorrhiza* 16(5):299–363.
8. Çakan H, Karataş Ç (2006) Interactions between mycorrhizal colonization and plant life forms along the successional gradient of coastal sand dunes in the eastern Mediterranean, Turkey. *Ecol Res* 21(2):301–310.
9. Fracchia S, et al. (2009) Mycorrhizal status of plant species in the Chaco Serrano Woodland from central Argentina. *Mycorrhiza* 19(3):205–214.
10. Birhane E, Kuyper TW, Sterck FJ, Bongers F (2010) Arbuscular mycorrhizal associations in Boswellia papyrifera (frankincense-tree) dominated dry deciduous woodlands of Northern Ethiopia. *For Ecol Manage* 260(12):2160–2169.
11. Fracchia S, Krapovickas L, Aranda-Rickert A, Valentinuzzi VS (2011) Dispersal of arbuscular mycorrhizal fungi and dark septate endophytes by Ctenomys cf. knighti (Rodentia) in the northern Monte Desert of Argentina. *J Arid Environ* 75(11):1016–1023.
12. N. A. Onguene (2011) Growth response of Pterocarpus soyauxii and Lophira alata seedlings to host soil mycorrhizal inocula in relation to land use types. *African J Microbiol Res* 5(17). doi:10.5897/AJMR10.061.
13. Perrier N, Amir H, Colin F (2006) Occurrence of mycorrhizal symbioses in the metal-rich lateritic soils of the Koniambo Massif, New Caledonia. *Mycorrhiza* 16(7):449–458.
14. Shi ZY, Feng G, Christie P, Li XL (2006) Arbuscular mycorrhizal status of spring ephemerals in the desert ecosystem of Junggar Basin, China. *Mycorrhiza* 16(4):269–275.
15. Tian C, Shi Z, Chen Z, Feng G (2006) Arbuscular mycorrhizal associations in the Gurbantunggut Desert. *Chinese Sci Bull* 51(S1):140–146.
16. Wu B, Isobe K, Ishii R (2004) Arbuscular mycorrhizal colonization of the dominant plant species in primary successional volcanic deserts on the Southeast slope of Mount Fuji. *Mycorrhiza* 14(6):391–395.
17. Menoyo E, Becerra AG, Renison D (2007) Mycorrhizal associations in Polylepis woodlands of Central Argentina. *Can J Bot* 85(5):526–531.
18. Roumet C, Urcelay C, Diaz S (2006) Suites of root traits differ between annual and perennial species growing in the field. *New Phytol* 170(2):357–368.
19. Lugo M, Cabello M (2002) Native arbuscular mycorrhizal fungi (AMF) from mountain grassland (Cordoba, Argentina) I. Seasonal variation of fungal spore diversity. *Mycologia* 94(4):579–586.
20. Urcelay C (2002) Co-occurrence of three fungal root symbionts in Gaultheria poeppiggi DC in Central Argentina. *Mycorrhiza* 12(2):89–92.
21. Nouhra ER, et al. (2008) Ocurrence of ectomycorrhizal, hypogeous fungi in plantations of exotic tree species in central Argentina. *Mycologia* 100(5):752–759.
22. KHAN AG (1978) VESICULAR-ARBUSCULAR MYCORRHIZAS IN PLANTS COLONIZING BLACK WASTES FROM BITUMINOUS COAL MINING IN THE ILLAWARRA REGION OF NEW SOUTH WALES. *New Phytol* 81(1):53–63.
23. Koske R, Gemma J, Flynn T (1992) Mycorrhizae in Hawaiian Angiosperms: A Survey with Implications for the Origin of the Native Flora. *Botany* 79(8):853–862.
24. Lugo MA, Negritto MA, Jofré M, Anton A, Galetto L (2012) Colonization of native Andean grasses by arbuscular mycorrhizal fungi in Puna: a matter of altitude, host photosynthetic pathway and host life cycles. *FEMS Microbiol Ecol* 81(2):455–466.
25. Cripps C, Eddington L (2005) Distribution of Mycorrhizal Types among Alpine Vascular Plant Families on the Beartooth Plateau, Rocky Mountains, U.S.A., in Reference to Large-Scale Patterns in Arctic-Alpine Habitats. *Arctic, Antarct Alp Res* 37(2):177–188.
26. Bâ AM, Duponnois R, Moyersoen B, Diédhiou AG (2012) Ectomycorrhizal symbiosis of tropical African trees. *Mycorrhiza* 22(1):1–29.

27. McGuire KL, et al. (2008) Dual mycorrhizal colonization of forest-dominating tropical trees and the mycorrhizal status of non-dominant tree and liana species. *Mycorrhiza* 18(4):217–222.
28. Peay KG, et al. (2015) Lack of host specificity leads to independent assortment of dipterocarps and ectomycorrhizal fungi across a soil fertility gradient. *Ecol Lett* 18(8):807–816.
29. Maksimova T (1985) Mykorizy gorno-tundrovyh rasteni Khakassii. *Mycorrhiza I Drugie Formy Konsortivnykh Svyasey v Prirode*, ed Selivanov I (Perm State University), pp 16–21.
30. Shkraba E (1987) Mykosymbiotrophism rasteni moggevelovyh lesov Tyan'-Shan'ya. *Mycorrhiza I Drugie Formy Konsortivnykh Svyasey v Prirode*, ed Selivanov IA (Perm State University), pp 8–20.
31. Boyle B, et al. (2013) The taxonomic name resolution service: an online tool for automated standardization of plant names. *BMC Bioinformatics* 14(1):16.
32. The Plant List (2013). Version 1.1.
33. van der Heijden MGA, Martin FM, Selosse M-A, Sanders IR (2015) Mycorrhizal ecology and evolution: the past, the present, and the future. *New Phytol* 205(4):1406–1423.
34. Zanne AE, et al. (2014) Three keys to the radiation of angiosperms into freezing environments. *Nature* 506(7486):89–92.
35. Beaulieu JM, O'Meara BC, Donoghue MJ (2013) Identifying hidden rate changes in the evolution of a binary morphological character: the evolution of plant habit in campanulid angiosperms. *Syst Biol* 62(5):725–37.
36. Wagenmakers E-J, Farrell S (2004) AIC model selection using Akaike weights. *Psychon Bull Rev* 11(1):192–6.
37. Yang Z (2006) *Computational Molecular Evolution* (Oxford University Press, Oxford, UK).
38. Remy W, Taylor TN, Hass H, Kerp H (1994) Four hundred-million-year-old vesicular arbuscular mycorrhizae. *Proc Natl Acad Sci* 91(25):11841–3.
39. Redecker D (2000) Glomalean Fungi from the Ordovician. *Science (80-)* 289(5486):1920–1921.
40. Taylor TN, Remy W, Hass H, Kerp H (1995) Fossil Arbuscular Mycorrhizae from the Early Devonian. *Mycologia* 87(4):560.
41. Maherali H, Oberle B, Stevens PF, Cornwell WK, McGlinn DJ (2016) Mutualism Persistence and Abandonment during the Evolution of the Mycorrhizal Symbiosis. *Am Nat* 188(5):E113–E125.
42. Delaux P-M, et al. (2015) Algal ancestor of land plants was preadapted for symbiosis. *Proc Natl Acad Sci* 112(43):13390–13395.
43. Bravo A, York T, Pumplin N, Mueller LA, Harrison MJ (2016) Genes conserved for arbuscular mycorrhizal symbiosis identified through phylogenomics. *Nat Plants* 2(2):15208.
44. Werner GDA, Cornwell WK, Sprent JI, Kattge J, Kiers ET (2014) A single evolutionary innovation drives the deep evolution of symbiotic N2-fixation in angiosperms. *Nat Commun* 5:4087.
45. Ellison AM, Gotelli NJ (2003) Evolutionary ecology of carnivorous plants. *Trends Ecol Evol* 16(11):623–629.
46. Albert V, Williams S, Chase M (1992) Carnivorous plants: phylogeny and structural evolution. *Science (80-)* 257(5076):1491–1495.
47. Těšitel J (2016) Functional biology of parasitic plants : a review. *Plant Ecol Evol* 149(1):5–20.
48. Westwood JH, Yoder JI, Timko MP, DePamphilis CW (2010) The evolution of parasitism in plants. *Trends Plant Sci* 15(4):227–235.
49. Merckx VS (2013) *Mycoheterotrophy* ed Merckx V (Springer New York, New York, NY) doi:10.1007/978-1-4614-5209-6.
50. Neumann G, Martinoia E (2002) Cluster roots – an underground adaptation for survival in extreme environments. *Trends Plant Sci* 7(4):162–167.
51. Shane MW, Lambers H (2005) Cluster roots: A curiosity in context. *Plant Soil* 274(1–2):101–125.
52. Schlauer J (2015) Carnivorous Plant Database. Available at: http://www.omnisterra.com/bot/cp_home.cgi [Accessed May 27, 2016].
53. Givnish TJ (2015) New evidence on the origin of carnivorous plants. *Proc Natl Acad Sci* 112(1):10–11.
54. Chase MW, Christenhusz MJM, Sanders D, Fay MF (2009) Murderous plants: Victorian Gothic, Darwin and modern insights into vegetable carnivory. *Bot J Linn Soc* 161(4):329–356.
55. Schlauer J, Meijer W, Hansen B Parasitic Plants Database. *2012*. Available at: http://www.omnisterra.com/bot/cp_home.cgi [Accessed May 27, 2016].
56. Yoshida S, Cui S, Ichihashi Y, Shirasu K (2016) The Haustorium, a Specialized Invasive Organ in Parasitic Plants. *Annu Rev Plant Biol* 67:643–667.
57. Selosse MA, Roy M (2009) Green plants that feed on fungi: facts and questions about mixotrophy. *Trends Plant Sci* 14(2):64–70.
58. Skene KR (2000) Pattern Formation in Cluster Roots: Some Developmental and Evolutionary Considerations. *Ann Bot* 85(6):901–908.
59. Skene KR (1998) Cluster roots: some ecological considerations. *J Ecol* 86(6):1060–1064.

60. Shane MW, Cawthray GR, Cramer MD, Kuo J, Lambers H (2006) Specialized “dauciform” roots of Cyperaceae are structurally distinct, but functionally analogous with “cluster” roots. *Plant, Cell Environ* 29(10):1989–1999.
61. Soltis DE, et al. (1995) Chloroplast gene sequence data suggest a single origin of the predisposition for symbiotic nitrogen fixation in angiosperms. *Proc Natl Acad Sci* 92(7):2647–51.
62. Werner GDA, Cornwell WK, Cornelissen JHC, Kiers ET (2015) Evolutionary signals of symbiotic persistence in the legume–rhizobia mutualism. *Proc Natl Acad Sci* 112(33):10262–10269.
63. Shane MW, Dixon KW, Lambers H (2005) The occurrence of dauciform roots amongst Western Australian reeds, rushes and sedges, and the impact of phosphorus supply on dauciform-root development in Schoenus unispiculatus (Cyperaceae). *New Phytol* 165(3):887–898.
64. Pagel M (1994) Detecting Correlated Evolution on Phylogenies: A General Method for the Comparative Analysis of Discrete Characters. *Proc R Soc B Biol Sci* 255(1342):37–45.
65. Pagel M (1999) Inferring the historical patterns of biological evolution. *Nature* 401(October 1999):877–884.
66. FitzJohn RG (2012) Diversitree : comparative phylogenetic analyses of diversification in R. *Methods Ecol Evol* 3(6):1084–1092.
67. Delaux P-M, et al. (2014) Comparative Phylogenomics Uncovers the Impact of Symbiotic Associations on Host Genome Evolution. *PLoS Genet* 10(7):e1004487.

AM

No Yes

Pie Colours

- Stable Non−AM Class: Species without AM
- Stable Non−AM Class: Species with AM
- Labile Class: Species without AM
- Labile Class: Species with AM
- Stable AM Class: Species without AM
- Stable AM Class: Species with AM

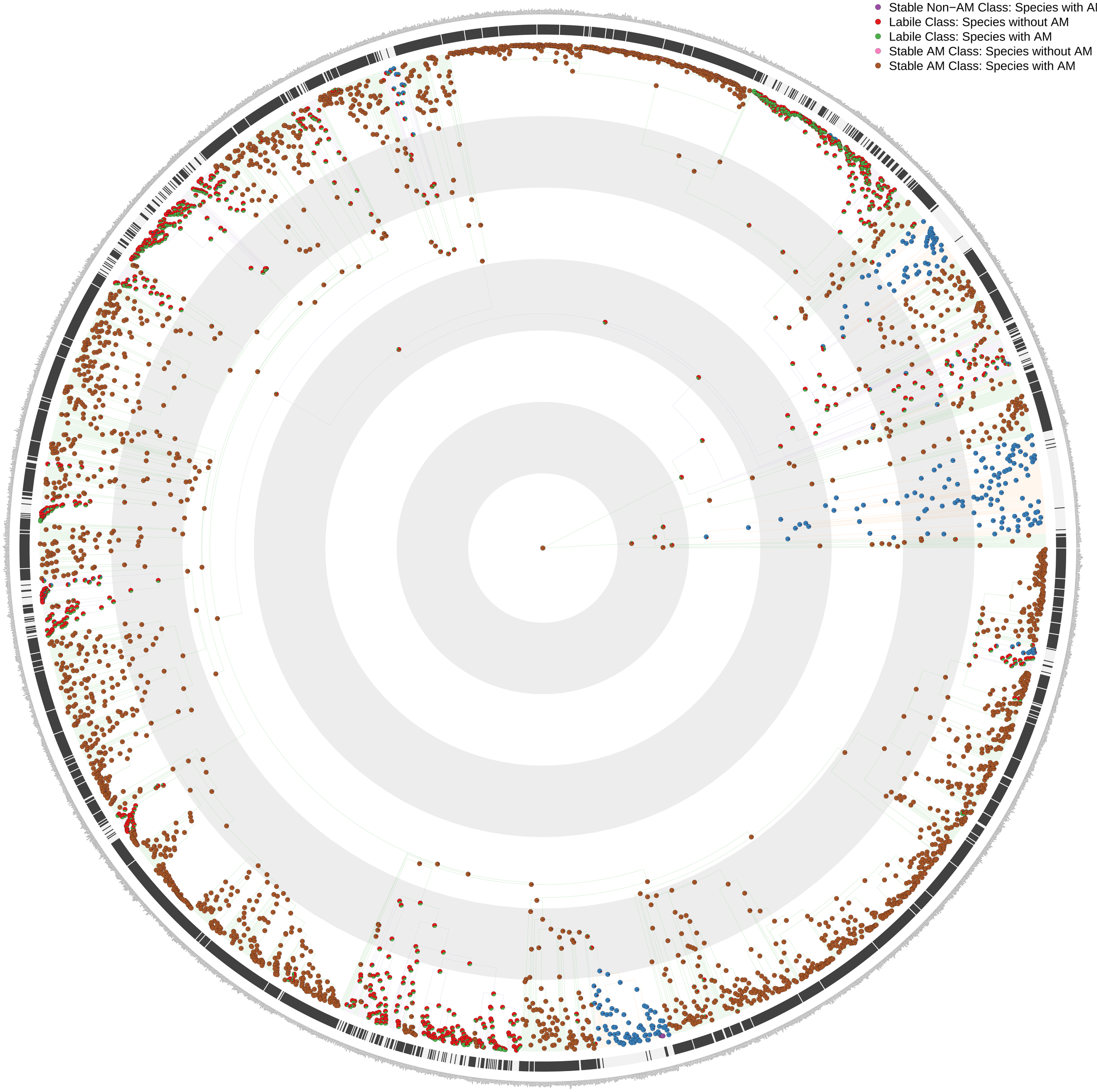

AM Fungi

No Yes

Other Symbionts

ECM ER / ARB N−fixation No ORM

Alternative Strategies
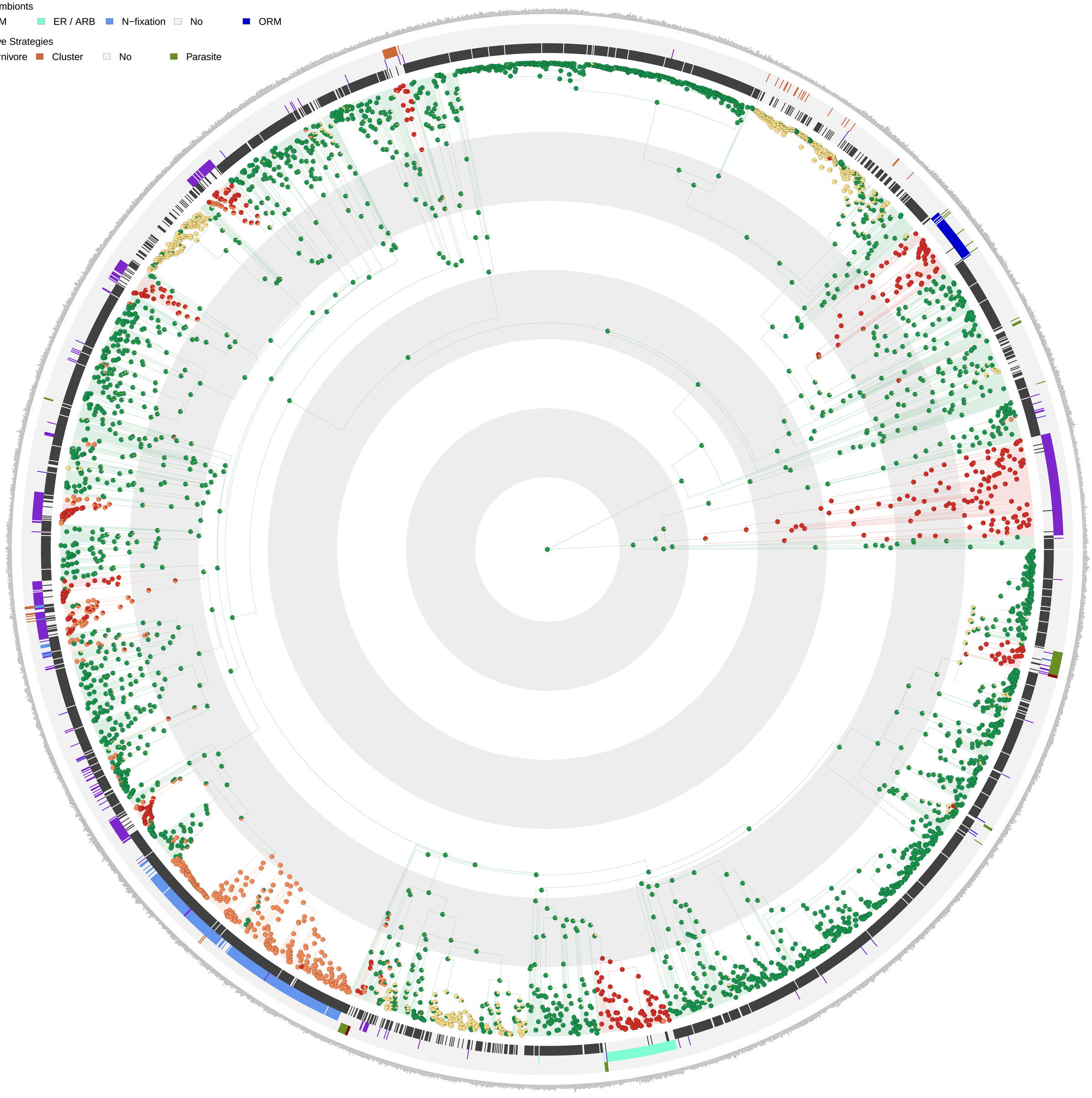
Carnivore Cluster No Parasite